Simple Shear Testing of Parallel-Fibered Planar Soft Tissues

John C. Gardiner

Jeffrey A. Weiss
e-mail: jeff.weiss@utah.edu

Department of Bioengineering,
The University of Utah,
50 South Central Campus Drive #2480,
Salt Lake City, UT 84112

The simple shear test may provide unique information regarding the material response of parallel-fibered soft tissues because it allows the elimination of the dominant fiber material response from the overall stresses. However, inhomogeneities in the strain field due to clamping and free edge effects have not been documented. The finite element method was used to study finite simple shear of simulated ligament material parallel to the fiber direction. The effects of aspect ratio, clamping prestrain, and bulk modulus were assessed using a transversely isotropic, hyperelastic material model. For certain geometries, there was a central area of uniform strain. An aspect ratio of 1:2 for the fiber to cross-fiber directions provided the largest region of uniform strain. The deformation was nearly isochoric for all bulk moduli indicating this test may be useful for isolating solid viscoelasticity from interstitial flow effects. Results suggest this test can be used to characterize the matrix properties for the type of materials examined in this study, and that planar measurements will suffice to characterize the strain. The test configuration may be useful for the study of matrix, fiber-matrix, and fiber-fiber material response in other types of parallel-fibered transversely isotropic soft tissues. [DOI: 10.1115/1.1351891]

1 Introduction

Collagenous soft tissues are subjected to complex three-dimensional deformations in vivo that may include tension, compression, and shear. The shear behavior affects load transfer between microstructural parts of the tissue. Accurate measurement of material coefficients that govern the shear behavior of soft tissue can improve the descriptive and predictive value of constitutive models. Quantification of the effects of disease or treatment on shear properties can provide insight into the relationship between different tissue components and continuum level shear behavior.

Finite simple shear is a homogeneous deformation consisting primarily of deviatoric strain. It is used as a canonical problem to highlight differences between infinitesimal and large strain theory, and to compare the response of different constitutive models. The deformation is applied in-plane to a relatively thin material sample (Fig. 1*A*). If the material is transversely isotropic and the local fiber direction is aligned with the shear direction, there will not be elongation along the fiber direction. This eliminates the normally dominant fiber material behavior from the tissue response to simple shear, providing an ideal method to investigate matrix properties, fiber-matrix, and fiber-fiber interactions. These data can augment tensile test data and help to identify an appropriate form for the matrix stress-strain behavior. Unlike the infinitesimal strain theory, finite simple shear cannot be maintained by shear stress alone (e.g., [1]). Normal stresses are needed to maintain the normal strains at zero. In the absence of normal stresses, the tissue will experience some contraction through the thickness and along the in-plane directions as shear strain is applied. This will result in an inhomogeneous strain field that cannot be predicted without additional analysis.

Infinitesimal cyclic shear loading has allowed the effects of strain rate and orientation to be quantified in biological soft tissues [2,3]. These studies applied infinitesimal strains as either simple or torsional shears. In contrast, Wilson et al. [4] subjected rabbit medial collateral ligament to inhomogeneous, large deformation shear loading during uniaxial tests by making lateral incisions that generated longitudinal shear planes. Results demonstrated that ligaments have a finite resistance to shear. Shear properties have also been investigated via tensile [5] or biaxial [6] tests with an oblique fiber direction. These techniques apply both shear and tension.

The finite simple shear test could provide unique information regarding the material response of planar, transversely isotropic soft tissues such as ligaments. However, strain field inhomogeneities in the experimental setting have never been quantified. Further, it is unclear if out-of-plane strains will be significant in these tests. Nonuniform strain fields could extend into the central portion of the test specimen, polluting the measured strains and making the assumption of a homogeneous deformation unreliable. Also, bulk properties could interact with clamping effects and sample dimensions. The objectives of this study were to examine finite simple shear of simulated ligament material using the finite element (FE) method. The effects of aspect ratio, clamping prestrain, and bulk modulus were assessed. It was hypothesized that complete characterization of the deformation within a central region of the tissue could be obtained using only planar measurements of strain, providing a protocol for future experimental studies of soft tissue shear properties.

2 Materials and Methods

The FE method was used to simulate a finite simple shear test of a planar sample of transversely isotropic material. The coordinate system in Fig. 1 is used throughout the following sections. Initial fiber direction was oriented along the *y*-axis. This orientation eliminates the fiber contribution—orientation of the fibers along the *x*-axis would result in the shear response being dominated by the fiber stress. Specimen dimensions and material properties were chosen to represent the human medial collateral ligament (MCL).

2.1 Comparison to Theoretical Solution. The Green-Lagrange shear (E_{XY}, E_{YZ}, and E_{XZ}) and normal strains (E_{XX}, E_{YY}, and E_{ZZ}) predicted by the FE simulations were compared to expected values for homogeneous simple shear. For simple shear parallel to the *y*-axis, the deformation gradient $\boldsymbol{F}$ can be determined from the shear angle θ between the *x*-axis and the top/bottom edges of the sample (Fig. 1*A*):

Contributed by the Bioengineering Division for publication in the JOURNAL OF BIOMECHANICAL ENGINEERING. Manuscript received by the Bioengineering Division Jan. 2000; revised manuscript received Dec. 2000. Associate Editor: L. A. Setton.

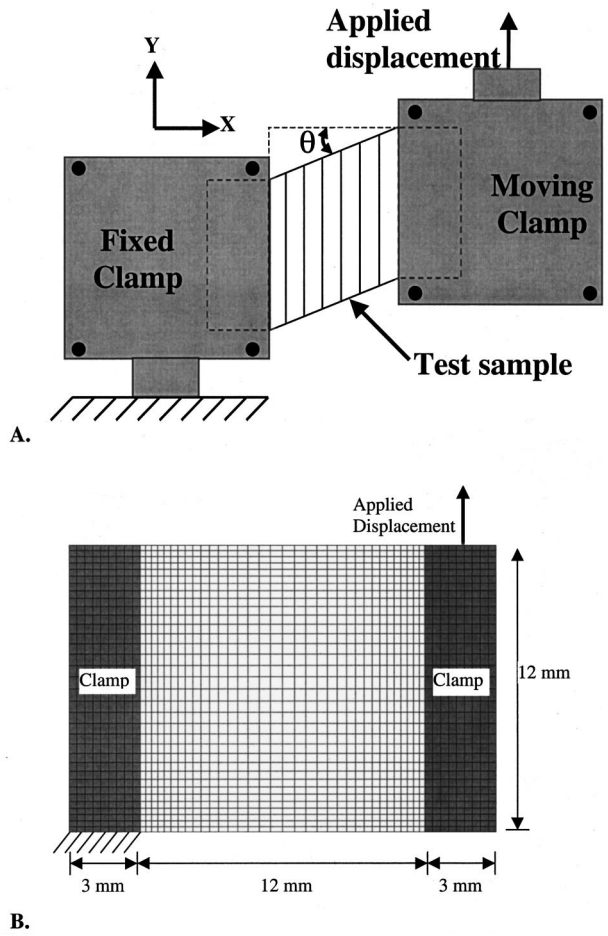

Fig. 1 ***A*—Schematic of simulated simple shear test configuration. Sample is gripped with two clamps and the right clamp is displaced vertically to induce a shear $\kappa=\tan(\theta)$, where θ is the angle between the *x*-axis and the top edge of the tissue. The coordinate axes illustrate the directions used to reference strain components, with the *z*-axis oriented out of the plane. *B*—Finite element mesh used for the 12×12 mm geometry. Four elements were used along the *z*-axis (out-of-plane) direction. Shaded regions indicate the areas of the tissue in the clamps.**

$$[\boldsymbol{F}]=\begin{bmatrix}1 & 0 & 0\\ \kappa & 1 & 0\\ 0 & 0 & 1\end{bmatrix} \tag{1}$$

Here, $\kappa=\tan(\theta)$. Because $\det(\boldsymbol{F})=1$, the deformation is isochoric (no volume change). The Green-Lagrange strain tensor $\boldsymbol{E}$ follows:

$$[\boldsymbol{E}]=\frac{1}{2}[\boldsymbol{F}^T\boldsymbol{F}-1]=\frac{1}{2}\begin{bmatrix}\kappa^2 & \kappa & 0\\ \kappa & 0 & 0\\ 0 & 0 & 0\end{bmatrix} \tag{2}$$

The only nonzero components of $\boldsymbol{E}$ should be E_{XY} and E_{XX}. When $\kappa=1/3$, these components should be $E_{XY}=0.167$ and $E_{XX}=0.055$.

2.2 Constitutive Model. The test sample was represented by a transversely isotropic hyperelastic material that has been used to describe and predict the behavior of ligaments and tendons [7–9]. The strain energy was

$$W=F_1(\tilde{I}_1)+F_2(\tilde{\lambda})+\frac{K}{2}[\ln(J)]^2 \tag{3}$$

where $\tilde{I}_1$ is the first deviatoric invariant, $\tilde{\lambda}$ is the deviatoric part of the stretch ratio along the local fiber direction, and $J=\det(\boldsymbol{F})$. The three terms represent the contribution from the matrix, the collagen fibers, and the tissue bulk response. The only nonzero strain energy derivative for the matrix strain energy F_1 was chosen so that $\partial F_1/\partial\tilde{I}_1=C_1$, yielding the relatively simple neo-Hookean constitutive model. In the limit of infinitesimal strains, C_1 has the interpretation of shear modulus. More complex representations of matrix behavior, such as the Mooney-Rivlin model, can be represented by introducing an additional strain energy dependency on the second deviatoric invariant, $\tilde{I}_2$ [9]. The function F_2 represents the strain energy from the fibers. It was assumed there was no dispersion in fiber orientation. Because the last term on the right-hand side of equation (3) represents the entire volumetric response of the material, the bulk behavior was controlled by the parameter *K*, referred to herein as the bulk modulus. The strain energy derivatives for the fibers were defined as a function of the fiber stretch:

$$\tilde{\lambda}\frac{\partial F_2}{\partial\lambda}=0,\quad \tilde{\lambda}<1,$$

$$\tilde{\lambda}\frac{\partial F_2}{\partial\lambda}=C_3[\exp(C_4(\tilde{\lambda}-1))-1],\quad 1<\tilde{\lambda}<\lambda^*, \tag{4}$$

$$\tilde{\lambda}\frac{\partial F_2}{\partial\lambda}=C_5\tilde{\lambda}+C_6,\quad \tilde{\lambda}\geqslant\lambda^*.$$

Here, C_3 scales the exponential stress, C_4 determines the rate of collagen uncrimping, C_5 is the modulus of the straightened collagen fibers, and λ^* is the fiber stretch at which the collagen is straightened. The theoretical solution predicts $\tilde{\lambda}=F_{22}=1$ and thus the collagen should not contribute to the stress. With the exception of bulk modulus, material properties were taken from a previous experimental study of MCL material behavior ($C_1=4.6$ MPa, $C_3=2.4$ MPa, $C_4=30.5$, $C_5=323.7$ MPa, $\lambda^*=1.055$) [10]. The effective bulk modulus was introduced as a study parameter.

2.3 Finite Element Analysis. A hexahedral FE mesh was constructed consisting of 7072 elements and 9275 nodes, with four elements through the thickness (Fig. 1*B*). Boundary conditions were applied through the nodes that were in contact with the clamps (Fig. 1*B*). The tissue extended 3 mm into each clamp and was assumed to be perfectly bonded to the clamp. Experimental loading was simulated in two phases. First, displacements were prescribed for nodes beneath the clamps to simulate tissue compression due to clamping (compression along *z*-axis in Fig. 1*A*). Second, a translation along the *y*-axis was prescribed to nodes contacting the right clamped surfaces to induce a shear of $\theta=\tan^{-1}(1/3)$. To simulate experimental conditions, the clamped surfaces were left unconstrained along the *x*-axis during application of clamping strain, but were constrained during application of shear strain.

Nonlinear FE analyses were performed using NIKE3D [11]. Three-field brick elements were used to avoid element locking for near-incompressible behavior [9]. Quasi-static analysis was used with the clamping strain applied from ''quasi-time'' $t=0.0$ to $t=1.0$, followed by application of shear strain from $t=1.0$ to $t=2.0$. An incremental-iterative solution strategy was used with a quasi-Newton procedure controlling the iterative process [12]. To determine the optimal configuration for shear testing, a series of parameter studies were performed.

2.4 Effect of Sample Geometry. Three geometries (*x*-*y* sample dimensions of 12×12, 6×12, and 12×6 mm) were analyzed with a bulk modulus of 1.0*e*4 MPa and clamping prestrains of 0 percent and 10 percent. These geometries represented the largest samples of relatively homogeneous tissue that could be harvested from human MCL and they allowed the effect of different aspect ratios on the strain fields to be assessed.

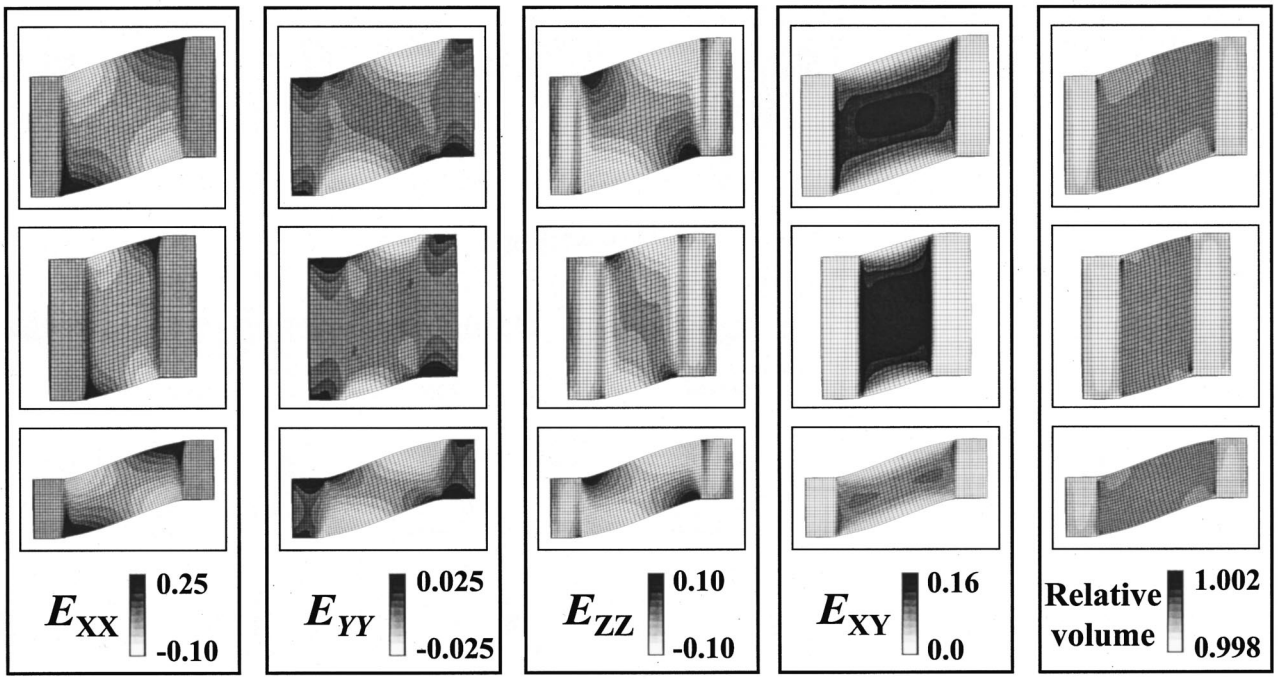

Fig. 2 Contours of Green-Lagrange strain and relative volume (V/V_0) for sample dimensions of 12×12 mm (top row), 6×12 mm (middle row), and 12×6 mm (bottom row). Note that the entire sample undergoes nearly isochoric deformation regardless of sample dimensions. Clamping prestrain=10 percent, $K=1.0e04$ MPa, $\tan(\theta)=1/3$.

2.5 Effect of Bulk Modulus. The bulk modulus was varied over four orders of magnitude using the 12×12 mm geometry and 10 percent clamping prestrain. In the analysis of rubber and other high polymers, if the effective bulk modulus is two or more orders of magnitude larger than the effective shear modulus, the material may be considered incompressible for all practical purposes [13]. Values of bulk modulus were chosen to be on the same order of magnitude as C_1, and then one, two, and three orders of magnitude larger than C_1 ($K=1.0e1$, $1.0e2$, $1.0e3$, and $1.0e4$ MPa).

2.6 Effect of Clamping Prestrain. The effect of clamping was studied at levels of 0, 5, 10, and 15 percent compressive prestrain for the 12×12 mm geometry with $K=1.0e4$ MPa. These levels of clamping represented a range between no clamping and the most clamping that cold be applied without element inversion during solution with the FE code.

For each analysis, the predicted Green-Lagrange strains (E_{XX}, E_{YY}, E_{XY}, E_{XZ}, E_{YZ}, and E_{ZZ}) and volume ratio [$J=\det(\boldsymbol{F})=V/V_0$] were examined at the sample center and compared to the theoretical solution [equation (2)]. The spatial distribution of strains and volume ratio were examined to determine areas of homogeneous strain and isochoric deformation.

3 Results

As clamping strain was applied, the tissue bulged toward the sample center and outside of the clamps. Because the clamps were free in the *x*-direction during the application of clamping prestrain, the bulging caused the clamps to move slightly apart. As shear was applied, effects from the free and clamped edges influenced the predicted strain and stress fields in the sample. The main area of positive E_{YY} strains was near the clamp edges (Fig. 2). Since positive E_{YY} strains were necessary to obtain positive fiber stretch λ, these are the areas where transverse isotropy contributed to the response. For all cases, the through-thickness shear strains (E_{YZ} and E_{ZX}) were essentially zero (<0.1 percent) except within approximately 1 mm of the clamped edges. Detailed results are described for each parameter study, while representative results are presented in graphical form (Figs. 2 and 3).

3.1 Effect of Sample Geometry. In the absence of clamping prestrain, the 12×12 and 6×12 mm geometries predicted the theoretical strains at the mesh center with good accuracy (Fig. 4). However, the E_{XY} strain for the 12×6 mm geometry became progressively lower than the predicted value with increasing shear strain. This was the case for the E_{XX} strain as well but to a lesser extent.

When 10 percent clamping prestrain was applied before the shear strain, the *x*-distance between the clamps increased and the strains near the clamp edges were altered. The strains at a distance greater than 1 or 2 mm from the clamps were essentially unaffected by clamping, with the exception of a small positive E_{ZZ} strain located throughout the central region of the sample due to the bulging effect. A 10 percent clamping prestrain resulted in tensile E_{ZZ} strains in the specimen center of 0.01, 0.05, and 0.16 percent for the 12×6, 12×12, and 6×12 mm geometries, respectively. Subsequent application of shear strain produced the opposite effect on the E_{ZZ} strain, with resulting values of −2.40, −0.56, and 0.01 percent for the 12×6, 12×12, and 6×12 geometries, respectively (Fig. 2, column 1). Following application of both clamping prestrain and shear strain, all geometries experienced alteration in the central region strains due to clamping and free edge effects (Fig. 2). The size of the central region of homogeneous strain was greatly affected by sample geometry (Fig. 3). For the 12×12 mm geometry, the E_{XY}, E_{XX}, E_{YY}, and E_{ZZ} strains varied over the sample, but there was a core area of approximately 5×2 mm in which the strains were homogeneous. The region of homogeneous strains increased to approximately 4×5 mm for the 6×12 mm geometry (Fig. 3). Within these homogeneous regions, the E_{XX} and E_{XY} strains for the 12×12 and 6×12 mm corresponded well with the theoretical strains of Fig. 4. The 12×6 mm geometry predicted E_{XY} and E_{XX} strains below the theoretical level (Fig. 2), however there was still a small central region over which this level was homogeneous. The homogeneous region for the 12×6 mm geometry was limited by the E_{XX} and the E_{ZZ} strain to an area of only approximately 2×2 mm (Fig. 3). For all geometries, the out of plane shear strains E_{YZ} and E_{ZX} were

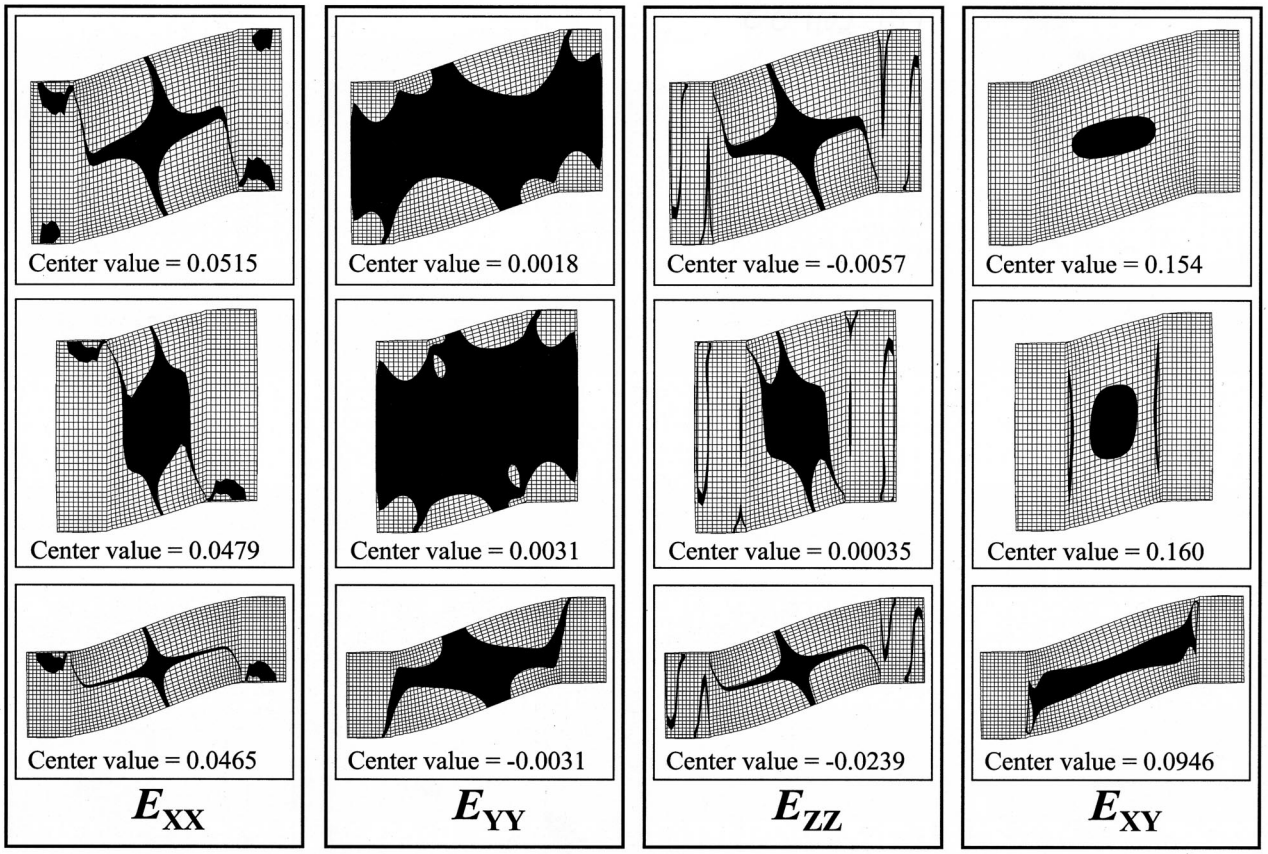

Fig. 3 Regions of homogeneous Green-Lagrange strain distribution for sample dimensions of 12×12 mm (top row), 6×12 mm (middle row), and 12×6 mm (bottom row). Black areas indicate regions of strains that correspond to ±0.005 of the indicated center value. Clamping prestrain=10 percent, K=1.0e04 MPa, tan(θ)=1/3.

essentially zero over the entire specimen. Regardless of sample geometry, the deformation was isochoric over the vast majority of the sample (Fig. 2, column 5).

3.2 Effect of Bulk Modulus. The main effect of bulk modulus was observed during application of clamping prestrain. As the bulk modulus was increased for the 12×12 mm sample, an increased amount of bulging of the tissue towards the sample center occurred resulting in a small increase in the amount of E_{ZZ} strain at the sample center. E_{ZZ} strains of 0.01, 0.007, 0.05, and 0.06 percent were observed following clamping prestrain for bulk moduli of 1.0e1, 1.0e2, 1.0e3, and 1.0e4 MPa, respectively. Increasing bulk modulus resulted in an increased x-displacement during clamping (0.081, 0.176, 0.246, and 0.259 mm for bulk moduli of 1.0e1, 1.0e2, 1.0e3, and 1.0e4 MPa, respectively) which induced little change in strains at the specimen center. With subsequent application of shear strain, the bulk modulus had virtually no effect on the predicted E_{XX} and E_{XY} strains at the center, with results remaining nearly identical to those depicted in Fig. 2. The volume ratio at the center was 1.0220, 1.0041, 1.0004, and 1.0000 for bulk moduli of 1.0e1, 1.0e2, 1.0e3, and 1.0e4 MPa, respectively, indicating that the deformation was nearly isochoric regardless of bulk modulus.

3.3 Effect of Clamping Prestrain. There was virtually no change in strain at the specimen center with variations in clamping prestrain. Increases in clamping prestrain caused an increase in E_{ZZ}, however, the effects were isolated to near the clamps. The main effect of increased prestrain was increased clamp x-displacement and strain alterations that were isolated to the clamped region.

4 Discussion

This study analyzed finite simple shear testing of planar, transversely isotropic biological soft tissues using the finite element method. Parameter studies assessed the sensitivity of the strain field to changes in geometry, bulk modulus, and clamping prestrain. Although the geometry and material properties used in the simulations represented the human MCL, the modeling technique may be used to examine the simple shear response of other constitutive models with homogenous fiber orientation.

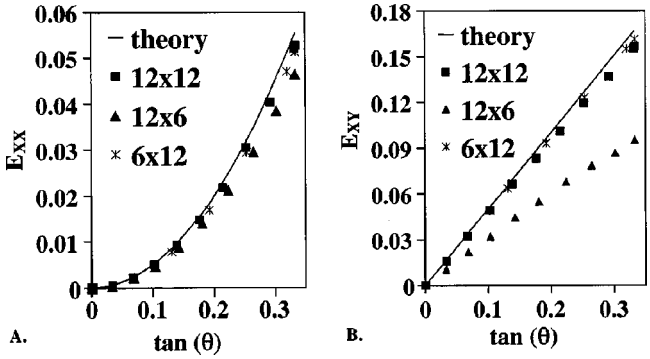

Fig. 4 Effect of specimen geometry on predicted Green-Lagrange components of shear (E_{XY}) and normal (E_{XX}) strain, as a function of shear angle applied to the clamps. Clamping prestrain=0 percent, K=1.0e04 MPa.

Sample geometry had the largest influence on strain field, and the effect was directly related to the relative proximity of the clamps and free edges to the specimen center. The 6×12 and 12×12 mm geometries reproduced the theoretical E_{XX} and E_{XY} strains with the most fidelity. The 6×12 mm geometry had a slightly larger area of homogeneous strain than the 12×12 mm geometry. This was mainly due to the E_{XX} and the E_{ZZ} strains, which were sensitive to the proximity of the clamps and free edges to the sample center. The 6×12 mm geometry may provide the best compromise between these errors and still provide a sufficiently large homogeneous central region for attachment of fiducial markers for strain measurement.

Variations in bulk modulus of four orders of magnitude induced virtually no change in relative volume near the specimen center. Regardless of geometry, bulk modulus, and clamping prestrain, the deformation was nearly isochoric over a large area. This indicated that simple shear provides an ideal method for studying solid matrix viscoelasticity. The isochoric nature of the deformation allows intrinsic matrix viscoelasticity to be separated from interstitial fluid flow.

The shear strains E_{YZ} and E_{ZX} were negligible in the same areas over which the deformation was isochoric. However, clamping prestrain and subsequent application of shear strain caused a small nonzero E_{ZZ} strain for the 12×12 and 12×6 geometries and a value near zero for the 6×12 geometry. These results imply that two-dimensional strain measurements may be used to characterize the deformation in a central region of the sample during finite simple shear. With marker-based measurement techniques, it is straightforward to determine the in-plane components of the deformation gradient, F_{xX}, F_{xY}, F_{yX}, and F_{yY} (e.g., [14]). If $\det(\boldsymbol{F})=1$,

$$\det[\boldsymbol{F}]=\det\begin{pmatrix} F_{xX} & F_{xY} & 0 \\ F_{yX} & F_{yY} & 0 \\ 0 & 0 & F_{zZ} \end{pmatrix}=1\Rightarrow F_{zZ}=\frac{1}{F_{xX}F_{yY}-F_{xY}F_{yX}} \tag{5}$$

Thus, the entire deformation gradient can be determined from two-dimensional measurements, assuming that (1) through-thickness shear strains E_{YZ} and E_{ZX} are negligible, and (2) deformation in the central region is homogeneous over the measurement area. The first assumption was valid for all cases examined, while the validity of the second assumption depended on specimen geometry. The solution in the central region does not have to correspond to the theoretical solution predicted by equation (2), as long as equation (5) applies over a large enough region.

One of the goals of material testing is to determine coefficients for a specified constitutive model. If a material undergoes homogeneous deformation and the constitutive law is known a priori, it is straightforward to estimate material coefficients (C_i) based on measurements of stress and strain using a nonlinear least-squares method. Although a homogeneous deformation may be generated over a central region during finite simple shear, edge effects preclude homogeneous deformation over an entire cross-section (Fig. 3). This prevents accurate measurement of local tissue stress levels from clamp measurements of force and thereby prevents the simple estimation of material coefficients. Use of the inverse FE method can circumvent this problem. By estimating an initial set of C_i, the FE method is used to predict the resultant clamp forces and strain field at the sample center for a given level of shear strain. The C_i are then iteratively updated until the FE predicted clamp forces and strain data match experimental measurements.

The rectangular specimen dimensions simulated in this study are easily created in an experimental setting by using steel punches to cut regular sample geometries from larger pieces of tissue [10,15]. Although the specific dimensions represented test samples of human MCL, other planar, parallel-fibered soft tissues can be prepared with similar aspect ratios. Tissues such as fascia lata and virtually any tendon would seem especially appropriate. If spatial variations in tissue thickness are large, they could affect the predicted results. Thickness variations could easily be incorporated into specimen-specific finite element models for parameter estimation.

A secure bond between the tissue and the clamps can be challenging to achieve experimentally. Tissue slippage or failure at the clamps has been reported during tensile failure tests performed along the fiber direction. For the sub-failure shear loading of this study, the loads in both the *x*- and *y*-directions are quite small (always less than 10 N in the simulations), suggesting that reactions at the clamps will not be sufficiently large to cause slippage or failure. Gripping techniques such as serrated gripping surfaces, the use of sandpaper or cyanoacrylate, or freeze-clamping could be incorporated if slippage presented a problem. These techniques can also minimize the amount of clamping prestrain that is necessary to adequately secure the tissue. Although a clamping prestrain of 10 percent had little effect on the resulting strain distribution at the center of the sample, larger values of prestrain could have a greater influence.

The predicted tissue response is only valid for the specific material model used for these simulations. The model did not include fiber-matrix or fiber-fiber interaction terms. The appropriate form and significance of these terms are currently unknown for most soft tissues. The model did not explicitly incorporate dispersion in the fiber angle of the material. The effects of such dispersion are unknown, although they could be assessed if an appropriate constitutive model and material coefficients were available to describe the dispersion. The effects of transverse isotropy on the predicted strains were isolated to areas near the clamps where the fiber stretch was greater than 1.0. Other models of transverse isotropy may have different effects on the observed strain fields. Specifically, the constitutive model used in this study was isotropic in compression, so a model with transverse isotropy in compression could produce different results. The simple shear test procedure provides a means to formulate a more sophisticated matrix model for description of the nonlinear material behavior observed for large deformation shear [5,6,15]. Although fiber angle dispersion was not studied in the present work, the same finite element modeling techniques can be used to assess the effects of fiber angle dispersion on predicted response.

In summary, finite deformation simple shear of a parallel-fibered, transversely isotropic hyperelastic material was analyzed using the finite element method. When fibers were oriented along the shear direction, this configuration allowed characterization of matrix shear properties without the influence of the fibers. Sample geometry had the largest effect on the strain field, while clamping prestrain and bulk modulus caused only small changes. An *x*-*y* aspect ratio of 1:2 provides the largest area of homogeneous strains, followed by an aspect ratio of 1:1. For these geometries, two-dimensional measurements of strain are sufficient to completely characterize the applied deformation in a central region of the test specimen. The present approach allows for the direct application of shear strain using a uniaxial test machine, without the assumptions of incompressibility or in-plane deformations. This provides the ability to characterize certain transversely isotropic compressible materials under shear without biaxial testing equipment.

Acknowledgments

Support by Whitaker Foundation Biomedical Research and Transition Grants is gratefully acknowledged.

References

[1] Marsden, J. E., and Hughes, T. J. R., 1983, *Mathematical Foundations of Elasticity*, Dover, New York.
[2] Anderson, D. R., Woo, S. L.-Y., Kwan, M. K., and Gershuni, D. H., 1991, ''Viscoelastic Shear Properties of the Equine Medial Meniscus,'' J. Orthop. Res., **9**, No. 4, pp. 550–558.
[3] Zhu, W., Mow, V. C., Koob, T. J., and Eyre, D. R., 1993, ''Viscoelastic Shear

Properties of Articular Cartilage and the Effects of Glycosidase Treatments,'' J. Orthop. Res., **11**, pp. 771–781.
[4] Wilson, A., Shelton, F., Chaput, C., Frank, C., Butler, D., and Shrive, N., 1997, ''The Shear Behavior of the Rabbit Medial Collateral Ligament,'' Med. Eng. Phys., **19**, No. 7, pp. 652–657.
[5] Goertzen, D. J., Budney, D. R., and Cinats, J. G., 1997, ''Methodology and Apparatus to Determine Material Properties of the Knee Joint Meniscus,'' Med. Eng. Phys., **19**, No. 5, pp. 412–419.
[6] Sacks, M. S., 1999, ''A Method for Planar Biaxial Mechanical Testing That Includes In-Plane Shear,'' ASME J. Biomech. Eng., **121**, pp. 551–555.
[7] Puso, M. A., and Weiss, J. A., 1998, ''Finite Element Implementation of Anisotropic Quasilinear Viscoelasticity,'' ASME J. Biomech. Eng., **120**, No. 1, pp. 62–70.
[8] Weiss, J. A., 1994, ''A Constitutive Model and Finite Element Representation for Transversely Isotropic Soft Tissues,'' Ph.D. thesis, University of Utah, Salt Lake City, UT.
[9] Weiss, J. A., Maker, B. N., and Govindjee, S., 1996, ''Finite Element Implementation of Incompressible, Transversely Isotropic Hyperelasticity,'' Comput. Methods Appl. Mech. Eng., **135**, pp. 107–128.
[10] Quapp, K. M., and Weiss, J. A., 1998, ''Material Characterization of Human Medial Collateral Ligament,'' ASME J. Biomech. Eng., **120**, pp. 757–763.
[11] Maker, B. N., Ferencz, R. M., and Hallquist, J. O., 1990, ''NIKE3D: A Non-Linear, Implicit, Three-Dimensional Finite Element Code for Solid and Structural Mechanics,'' Lawrence Livermore National Laboratory Technical Report, UCRL-MA-105268.
[12] Matthies, H., and Strang, G., 1979, ''The Solution of Nonlinear Finite Element Equations,'' Int. J. Numer. Methods Eng., **14**, pp. 1613–1626.
[13] Ogden, R. W., 1984, *Nonlinear Elastic Deformations*, Dover, New York.
[14] Sacks, M., and Choung, C., 1998, ''Orthotropic Mechanical Properties of Chemically Treated Bovine Pericardium,'' Ann. Biomed. Eng., **26**, pp. 892–902.
[15] Gardiner, J., Cordaro, N., and Weiss, J., 2000, ''Elastic and Viscoelastic Shear Properties of the Medial Collateral Ligament,'' *Trans 46th Annual Orthopaedic Research Society Meeting*, Vol. 25, p. 63.